



# Antibiotic Resistance in *Vibrio cholerae*: Mechanistic Insights from IncC Plasmid-Mediated Dissemination of a Novel Family of Genomic Islands Inserted at *trmE*

 Nicolas Rivard,<sup>a</sup>  Rita R. Colwell,<sup>b,c,d</sup>  Vincent Burrus<sup>a</sup>

<sup>a</sup>Département de Biologie, Université de Sherbrooke, Sherbrooke, Québec, Canada

<sup>b</sup>Maryland Pathogen Research Institute, University of Maryland, College Park, Maryland, USA

<sup>c</sup>John Hopkins Bloomberg School of Public Health, John Hopkins University, Baltimore, Maryland, USA

<sup>d</sup>Center for Bioinformatics and Computational Biology, University of Maryland, College Park, Maryland, USA

**ABSTRACT** Cholera remains a formidable disease, and reports of multidrug-resistant strains of the causative agent *Vibrio cholerae* have become common during the last 3 decades. The pervasiveness of resistance determinants has largely been ascribed to mobile genetic elements, including SXT/R391 integrative conjugative elements, IncC plasmids, and genomic islands (GIs). Conjugative transfer of IncC plasmids is activated by the master activator AcaCD whose regulatory network extends to chromosomally integrated GIs. MGIVchHai6 is a multidrug resistance GI integrated at the 3' end of *trmE* (*mmE* or *thdF*) in chromosome 1 of non-O1/non-O139 *V. cholerae* clinical isolates from the 2010 Haitian cholera outbreak. In the presence of an IncC plasmid expressing AcaCD, MGIVchHai6 excises from the chromosome and transfers at high frequency. Herein, the mechanism of mobilization of MGIVchHai6 GIs by IncC plasmids was dissected. Our results show that AcaCD drives expression of GI-borne genes, including *xis* and *mobI<sub>M</sub>*, involved in excision and mobilization. A 49-bp fragment upstream of *mobI<sub>M</sub>* was found to serve as the minimal origin of transfer (*oriT*) of MGIVchHai6. The direction of transfer initiated at *oriT* was determined using IncC plasmid-driven mobilization of chromosomal markers via MGIVchHai6. In addition, IncC plasmid-encoded factors, including the relaxase Tral, were found to be required for GI transfer. Finally, *in silico* exploration of *Gammaproteobacteria* genomes identified 47 novel related and potentially AcaCD-responsive GIs in 13 different genera. Despite sharing conserved features, these GIs integrate at *trmE*, *yicC*, or *dusA* and carry a diverse cargo of genes involved in phage resistance.

**IMPORTANCE** The increasing association of the etiological agent of cholera, *Vibrio cholerae* serogroup O1 and O139, with multiple antibiotic resistance threatens to deprive health practitioners of this effective tool. Drug resistance in cholera results mainly from acquisition of mobile genetic elements. Genomic islands conferring multidrug resistance and mobilizable by IncC conjugative plasmids were reported to circulate in non-O1/non-O139 *V. cholerae* clinical strains isolated from the 2010 Haitian cholera outbreak. As these genomic islands can be transmitted to pandemic *V. cholerae* serogroups, their mechanism of transmission needed to be investigated. Our research revealed plasmid- and genomic island-encoded factors required for the resistance island excision, mobilization, and integration, as well as regulation of these functions. The discovery of related genomic islands carrying diverse phage resistance genes but lacking antibiotic resistance-conferring genes in a wide range of marine dwelling bacteria suggests that these elements are ancient and recently acquired drug resistance genes.

**KEYWORDS** antibiotic resistance, IncC plasmids, mobilization, relaxase, T4CP, T4SS, *Vibrio cholerae*, conjugation, genomic islands, horizontal gene transfer, *oriT*, phage resistance

**Citation** Rivard N, Colwell RR, Burrus V. 2020. Antibiotic resistance in *Vibrio cholerae*: mechanistic insights from IncC plasmid-mediated dissemination of a novel family of genomic islands inserted at *trmE*. mSphere 5:e00748-20. <https://doi.org/10.1128/mSphere.00748-20>.

**Editor** Mariana Castanheira, JMI Laboratories

**Copyright** © 2020 Rivard et al. This is an open-access article distributed under the terms of the [Creative Commons Attribution 4.0 International license](https://creativecommons.org/licenses/by/4.0/).

Address correspondence to Vincent Burrus, [vincent.burrus@usherbrooke.ca](mailto:vincent.burrus@usherbrooke.ca).

**Received** 28 July 2020

**Accepted** 11 August 2020

**Published** 26 August 2020

Cholera is an acute diarrheal disease that leads to severe dehydration and often death in the absence of adequate treatment (1). The seventh cholera pandemic, which began in 1961, is caused by toxigenic strains of the *Gammaproteobacteria* *Vibrio cholerae* serogroup O1 biotype El Tor, or more sporadically its O139 variant (1). Since the late 1980s, antibiotic-resistant *V. cholerae* strains have emerged and spread globally (2). Development of drug resistance in seventh pandemic *V. cholerae* has been ascribed to mutation but it mostly involves acquisition of mobile genetic elements, including genomic island GI-15, integrative conjugative elements of the SXT/R391 family, and conjugative plasmids of incompatibility group C (IncC) (3–5).

IncC plasmids are large (>120-kbp) broad-host-range conjugative plasmids frequently associated with multidrug resistance in several species of globally distributed pathogenic enterobacteria, and in seventh pandemic *V. cholerae* strains from Africa, China, and Haiti (4, 6–8). Conjugative transfer of IncC plasmids is controlled by the FlhCD-like heteromeric transcriptional activator AcaCD that they encode (9). AcaCD activates 17 promoters conserved in IncC plasmids, including those driving expression of transfer genes and operons encoding type IV secretion system (T4SS) and conjugative pilus, relaxase Tral, putative type IV coupling protein (T4CP) TraD, and unknown function protein TraJ (9). Tral belongs to the MOB<sub>H1</sub> family of relaxases, and together with the product of *mobl<sub>C</sub>*, is essential for initiation of conjugative transfer at the origin of transfer (*oriT*) (10, 11). *Mobl<sub>C</sub>* is responsible for recognition of the *oriT* locus of IncC plasmids that is located immediately upstream of *mobl<sub>C</sub>* (12). Unlike other transfer genes, *mobl<sub>C</sub>* seems to be expressed in an AcaCD-independent manner (9).

Furthermore, AcaCD also triggers excision of at least three types of genomic islands (GIs) shown to be mobilizable in *trans* by IncC plasmids. The first type, integrated at the 3' end of the gene of unknown function *yicC*, is exemplified by the 16.5-kbp MGIV*mi1* of *Vibrio mimicus* (9). The two other types of GIs are inserted into the 3' end of *trmE* (also known as *mnmE* or *thdF*), a gene encoding the 5-carboxymethylaminomethyl-uridine-tRNA synthase GTPase subunit (13, 14). One type of GI is illustrated by the 42.4-kbp *Salmonella* genomic island 1 (SGI1) that confers resistance to ampicillin, chloramphenicol, streptomycin/spectinomycin, sulfamethoxazole, and tetracycline (AC-SSuT) in *Salmonella enterica* (14, 15). The other is illustrated by the 47.4-kbp MGIV*chHai6* of *V. cholerae* HC-36A1 that confers not only the ACSSuT phenotype but also trimethoprim and possibly mercury resistance (Fig. 1A) (13). MGIV*chHai6* was found in non-O1/non-O139 *V. cholerae* strains isolated from patients exhibiting symptoms of cholera at the onset of the 2010 cholera outbreak in Haiti. Despite integrating into the same site as SGI1, MGIV*chHai6* encodes a distantly related integrase Int (67% identity) and recombination directionality factor (RDF) Xis (37% identity) (13). MGIV*chHai6* also lacks most of the genes and sequences that enable the mobilization of SGI1 by IncC plasmids (13, 16, 17). On the basis of these structural differences, the mechanisms of mobilization of MGIV*chHai6* and SGI1 by IncC plasmids are expected to differ considerably. In MGIV*chHai6*, *xis* is the last gene of a putative operon-like structure preceded by a putative AcaCD-controlled promoter (Fig. 1A). A second AcaCD binding site is located inside an open reading frame (ORF) that encodes a distant homolog of *Mobl<sub>C</sub>* (27% identity over two fragments of 109 and 53 amino acid residues) (13). Besides AcaCD, IncC plasmid- and GI-encoded factors involved in MGIV*chHai6* mobilization have not been characterized.

In this report, we established a model of mobilization of MGIV*chHai6* by helper IncC plasmids and compared this model to SGI1 mobilization. Deletion mutants of the helper plasmid and MGI were used in mating assays to characterize the contribution of each element in MGIV*chHai6* mobilization. The presence of AcaCD binding sites upstream of *xis* and inside the putative gene encoding a *Mobl<sub>C</sub>* homolog suggests the presence of AcaCD-responsive promoters that were verified using *lacZ* reporter fusions. By analogy with IncC plasmids, we hypothesized that the *Mobl<sub>C</sub>* homolog encoded by MGIV*chHai6* recognizes a cognate *oriT* locus located upstream of its gene. The ability of IncC plasmids to mobilize chromosomal DNA through MGIV*chHai6* was also tested and provided the directionality of transfer initiated at *oriT*. Finally, phylogenetic analyses

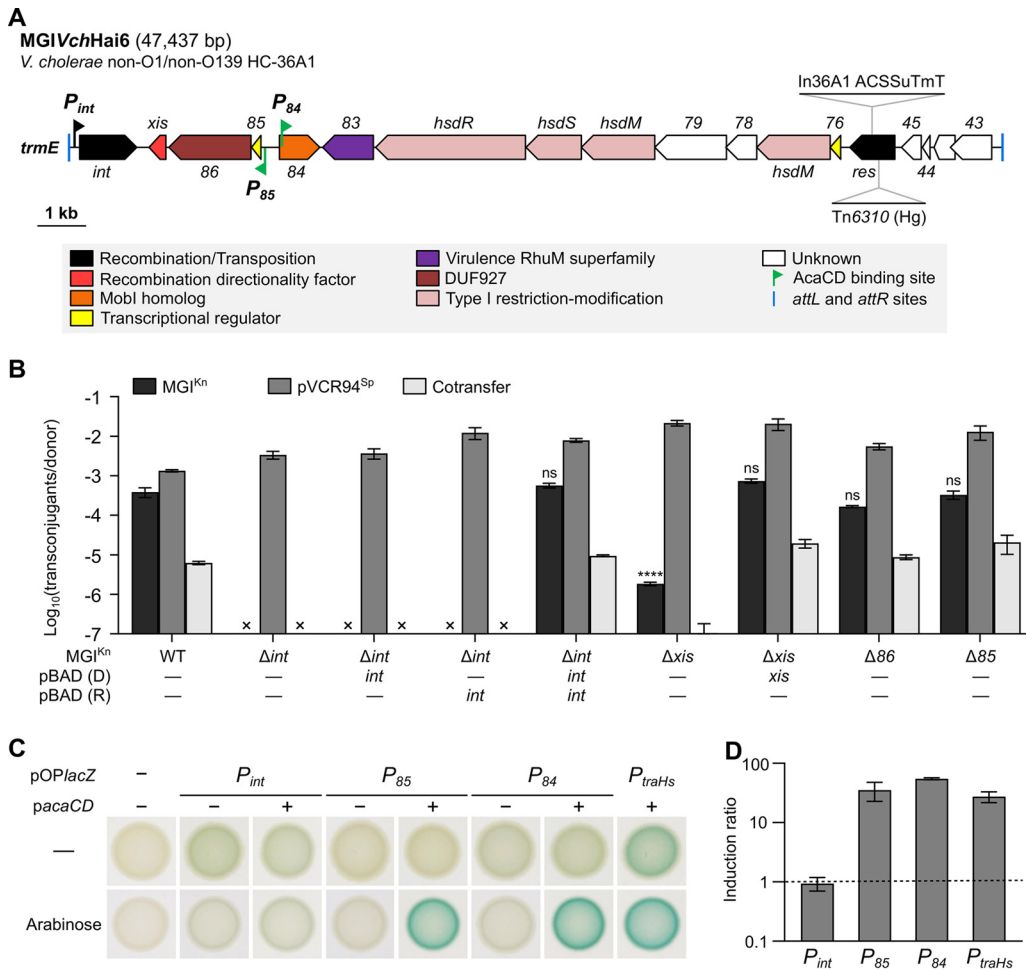


**FIG 1** Role and regulation of *int* and *85-86-xis* in the mobilization of MGIVchHai6. (A) Schematic genetic map of MGIVchHai6 drawn to scale. The left and right junctions (*attL* and *attR*) within the host chromosome are indicated by blue ticks at the extremities. ORFs with similar function are color coded as indicated in the figure. Green flags indicate the position and orientation of predicted AcaCD binding sites (13). The black flag indicates the position and orientation of the *P<sub>int</sub>* promoter. The insertion sites of In36A1 integron and Tn6310 transposon are shown. The gene numbers correspond to the last digits of the respective locus tags in GenBank accession no. [AXDR01000001](https://genbank.ncbi.nlm.nih.gov/GenBank/AXDR01000001). ACSSuTmT, resistance to ampicillin, chloramphenicol, spectinomycin/streptomycin, sulfamethoxazole, trimethoprim, and tetracycline; Hg, mercury resistance. (B) Mobilization assays of MGIV<sup>kn</sup> or its  $\Delta int$ ,  $\Delta xis$ ,  $\Delta 86$ , or  $\Delta 85$  mutants were carried out using *E. coli* GG56 (Nx) bearing pVCR94<sup>Sp</sup> as the donor strain, and CAG18439 (Tc) as the recipient strain. Complementation assays were performed in the donor (D) or recipient (R) strain by expressing the missing gene from *P<sub>BAD</sub>* on pBAD-*int* or pBAD-*xis*. An "x" indicates that the transfer frequency was below the detection limit ( $<10^{-7}$ ). Bars represent the means  $\pm$  standard errors of the means (error bars) from three independent experiments. Statistical analyses were carried out on the logarithm of the values using a one-way analysis of variance (ANOVA), followed by Dunnett's multiple-comparison test with the wild-type (WT) MGIV<sup>kn</sup> as the control. Statistical significance is indicated as follows: \*\*\*\*,  $P < 0.0001$ ; ns, not significant. (C)  $\beta$ -Galactosidase activities of *P<sub>int</sub>*, *P<sub>85</sub>*, and *P<sub>84</sub>* transcriptionally fused to *lacZ*. Colonies were grown on LB agar with or without arabinose to induce *acaCD* expression from *pacaCD*. (D) Induction levels of *P<sub>int</sub>*, *P<sub>85</sub>*, and *P<sub>84</sub>* in response to AcaCD.  $\beta$ -Galactosidase assays were carried out using the strains of panel C. Ratios between the enzymatic activities in Miller units for the arabinose-induced versus noninduced strains containing *pacaCD* are shown. The AcaCD-regulated promoter *P<sub>traHs</sub>* of SGI1 served as a positive control, and cells devoid of pOPlacZ served as a negative control. The bars represent the means  $\pm$  standard errors of the means (error bars) from two independent experiments.

based on the mobilization factor revealed the existence of a large class of potential IncC-mobilized GIs that are integrated at three different chromosomal sites in mostly marine dwelling species of *Gammaproteobacteria*. Our results show that MGIVchHai6-like GIs share a mechanism of mobilization by helper IncC plasmids that differs from the one used by SGI1-like GIs.

## RESULTS

***int* and *xis* are essential for excision and mobilization of MGIVchHai6.** MGIVchHai6 carries a large cargo of antibiotic and mercury resistance genes. To make it more

amenable for this study, we constructed a kanamycin (Kn)-resistant mutant of *MGIvch-Hai6* that lacks *In36A1*, *Tn6310*, and *res* (Fig. 1A). The resulting 19.5-kb mutant, named hereafter *MGI<sup>Kn</sup>*, was mobilized by the helper IncC plasmid *pVCR94<sup>SP</sup>* at the same frequency as *MGIvchHai6* ( $[5.2 \pm 0.3] \times 10^{-4}$  versus  $[5.7 \pm 1.2] \times 10^{-4}$ ,  $P = 0.622$ , Student's *t* test).

To establish whether *int* is required for mobilization of *MGIvchHai6*, we carried out mobilization assays using *pVCR94<sup>SP</sup>* and a  $\Delta int$  mutant of *MGI<sup>Kn</sup>*. Deletion of *int* abolished *MGI<sup>Kn</sup>* mobilization (Fig. 1B). Complementation assays done by expressing *int* from the arabinose-inducible promoter  $P_{BAD}$  on *pBAD-int* restored mobilization to the wild-type level only when *pBAD-int* was present in both the donor and recipient strains. Therefore, *int* is likely required for excision of *MGI<sup>Kn</sup>* in donor cells and for its integration into the chromosome of recipient cells.

The predicted (RDF) gene *xis* encodes a 114-amino-acid (aa)-residue protein containing a predicted helix-turn-helix (HTH\_17, Pfam accession no. PF12728) domain (position 39 to 89). To assess the role of *xis*, we mobilized the  $\Delta xis$  mutant of *MGI<sup>Kn</sup>* using *pVCR94<sup>SP</sup>*. Transfer of this mutant was reduced  $\sim 200$ -fold compared to the wild type (Fig. 1B). Complementation using *pBAD-xis* in donor cells was sufficient to restore the mobilization of *MGI<sup>Kn</sup>*  $\Delta xis$  to the wild-type level, thereby confirming that Xis is required only in donor cells, likely to facilitate Int-mediated excision of the GI.

*xis* is located downstream of two open reading frames (ORFs), *85* and *86* (the gene numbers correspond to the last digits of the respective locus tags in GenBank accession no. [AXDR01000001](#)), of unknown function. The predicted translation products of *85* is a 65-aa-residue protein that, like *xis*, contains an HTH\_17 domain (position 11 to 62). *86* encodes a predicted 558-aa-residue protein containing a domain of unknown function (DUF927, Pfam accession no. PF06048) in its N-terminal half. Mobilization assays using  $\Delta 85$  and  $\Delta 86$  mutants of *MGI<sup>Kn</sup>* and *pVCR94<sup>SP</sup>* revealed that neither *85* nor *86* is involved in the excision, mobilization, or integration of *MGI<sup>Kn</sup>* under laboratory conditions, as the frequency of mobilization remained unaffected by deletions (Fig. 1B).

To validate the involvement of *int* and *xis* in the excision step, we carried out PCR excision assays to detect the *attP* site on the plasmid-like form of excised *MGI<sup>Kn</sup>*, using *E. coli* GG56 (nalidixic acid) bearing *MGI<sup>Kn</sup>* or *MGI<sup>Kn</sup>*  $\Delta int$ . Spontaneous excision was undetectable, as shown by the absence of *attP* PCR product (see Fig. S1 in the supplemental material). Overexpression of *int* from  $P_{int}$  did not trigger excision, whereas overexpression of *xis* resulted in excision of *MGI<sup>Kn</sup>*, but not of *MGI<sup>Kn</sup>*  $\Delta int$ . Thus, excision of *MGIvchHai6* is induced by Xis and requires Int, in line with their proposed roles of RDF and integrase, respectively.

**AcaCD-dependent activation of mobility genes of *MGIvchHai6*.** AcaCD binding sites were previously detected upstream of *85* and inside *84* (13). To test whether AcaCD activates promoter sequences upstream of *int* and *85* or inside *84*,  $P_{int}$ ,  $P_{85}$ , and  $P_{84}$  were introduced upstream of a single-copy, chromosomal promoterless *lacZ* gene cassette that is transcriptionally isolated by the terminator sequences *rgnB* and *tl3* (9). The AcaCD-responsive promoter sequence  $P_{traHs}$  of SGI1 (17) was used as a positive control. The  $\beta$ -galactosidase activity of each promoter was monitored in the presence and absence of ectopically expressed *acaCD*.

$P_{int}$  yielded a weak yet constitutive  $\beta$ -galactosidase activity regardless of the presence of AcaCD (Fig. 1C), confirming that the promoter that drives expression of the integrase gene is not controlled by AcaCD. In contrast,  $P_{85}$ , which likely drives expression of the RDF gene *xis*, did not appear to produce detectable  $\beta$ -galactosidase activity in the absence of AcaCD (Fig. 1C). When *acaCD* was expressed,  $P_{85}$  activity increased 35-fold (Fig. 1D). Finally,  $P_{84}$  exhibited a weak, constitutive expression similar to  $P_{int}$  and weaker than  $P_{traHs}$  in the absence of AcaCD (Fig. 1C). Like  $P_{traHs}$ ,  $P_{84}$  was strongly induced (55-fold increase) upon expression of *acaCD* (Fig. 1D).

These results confirm that the two promoter sequences  $P_{85}$  and  $P_{84}$  containing the predicted AcaCD binding sites are activated by AcaCD. In contrast,  $P_{int}$  drives low-level constitutive expression of the integrase gene.

**MobI<sub>M</sub> is required for MGIVchHai6 mobilization.** The 795-bp open reading frame 84 (locus VCHC36A1\_0084 of *V. cholerae* HC-36A1) of MGIVchHai6 encodes a distant homolog of MobI<sub>C</sub> (27% identity). Since MobI<sub>C</sub> is a key factor for IncC plasmid transfer, we wondered whether 84 could play an important role in mobilization of MGIVchHai6. To test the hypothesis, we constructed MGIV<sup>Kn</sup> Δ84 and carried out mobilization assays with pVCR94<sup>SP</sup>. MGIV<sup>Kn</sup> transfer was strongly impaired by this deletion and reduced ~2,700-fold (Fig. 2A). In this context, we observed a slight (12-fold), yet statistically significant, increase of pVCR94<sup>SP</sup> transfer. Complementation of the Δ84 mutation from pBAD-84 restored MGIV<sup>Kn</sup> mobilization to the wild-type level, while reducing transfer of pVCR94<sup>SP</sup> ~40-fold, suggesting that 84 is essential for MGIVchHai6 mobilization. However, the position of the AcaCD-responsive  $P_{84}$  promoter inside 84 suggested that the protein effective for mobilization is smaller than predicted. To test this hypothesis, we constructed complementation plasmids containing fragments of 84 starting at the following alternative start codons: +31, GTG; +106, GTG; +118, ATG; +304, ATG; and +409, TTG (Fig. 2B). All plasmids but pBAD-84-304 and pBAD-84-409 restored mobilization of MGIV<sup>Kn</sup> Δ84 by pVCR94<sup>SP</sup> to the wild-type level (Fig. 2C). Therefore, the ORF located downstream of  $P_{84}$  and starting at ATG<sub>118</sub> in 84 is the likely gene that allows MGIVchHai6 mobilization. This gene, hereafter referred to as *mobI<sub>M</sub>*, produces a putative 225-aa-residue protein.

**Localization and characterization of the origin of transfer (*oriT*).** In IncC plasmids, *oriT* is located directly upstream of *mobI<sub>C</sub>* (10, 12). By analogy, we predict that *oriT* of MGIVchHai6 is located at the corresponding position, i.e., upstream of *mobI<sub>M</sub>*. To confirm this hypothesis, we first cloned the intergenic region located between 85 and 84 (*IG0*) as well as 84 into the low-copy-number nonmobilizable plasmid pDC1. The resulting plasmid, pIG0-84, was mobilized by pVCR94<sup>SP</sup> at a frequency comparable to that of MGIV<sup>Kn</sup> (Fig. 2D), thereby confirming the cloned fragment sufficient to support mobilization by the IncC plasmid even in the absence of MGIVchHai6. Site-directed mutagenesis G120C (ATG to ATC) and G306C (ATG to ATC) in 84 confirmed that ATG<sub>118</sub> is the start codon of *mobI<sub>M</sub>* since pIG0-84 carrying the mutation G120C was not mobilizable, whereas mutation G306C had no effect on transfer (Fig. 2D).

Since we were able to use pBAD-84-118 to complement and mobilize the Δ84 mutant of MGIV<sup>Kn</sup> that lacks the 117-bp segment containing the AcaCD-responsive promoter  $P_{84}$ , the possibility that *oriT* could be located in this sequence or in *mobI<sub>M</sub>* was ruled out. Therefore, we cloned *IG0* and the region extending upstream of *mobI<sub>M</sub>* (*IG10*) into pDC1 and carried out mobilization assays using pVCR94<sup>SP</sup> to provide the conjugative machinery. Donor cells also carried pT84 to provide MobI<sub>M</sub>. The empty vector and the same vector bearing *IG0* in the absence of pT84 were both unable to transfer (Fig. 3A). In contrast, when pT84 was present in donor cells, the vector bearing *IG10* or *IG0* transferred at frequencies that were comparable to that of MGIV<sup>Kn</sup> Δ84 complemented with pT84. This result indicated that *oriT* is located within *IG0*.

Insert reduction was then performed to find the minimal sequence of *IG0* allowing mobilization by pVCR94<sup>SP</sup>. The smallest insert capable of acting as a suitable *oriT*, *IG8*, was 49 bp long and located immediately upstream of 84 (Fig. 3A). Although functional, *IG8* provided only 1/10th of the mobilization activity of *IG0* or larger inserts such as *IG6* or *IG13* that provided additional upstream or downstream sequences. The addition of either 43 bp upstream (*IG6*) or 30 bp downstream (*IG13*) led to transfer frequencies equivalent to that obtained with *IG10*, and addition of both fragments (*IG12*) did not enhance transfer further. Predicted folding of *IG12* revealed three potential stem-loop structures within *IG8* and on either side, highlighting the presence of repeated sequences potentially involved in relaxosome assembly (Fig. 3B).

**Directionality of transfer initiated at *oriT*.** To determine the direction of conjugative transfer initiated at *oriT* of MGIVchHai6, chromosomal markers located upstream

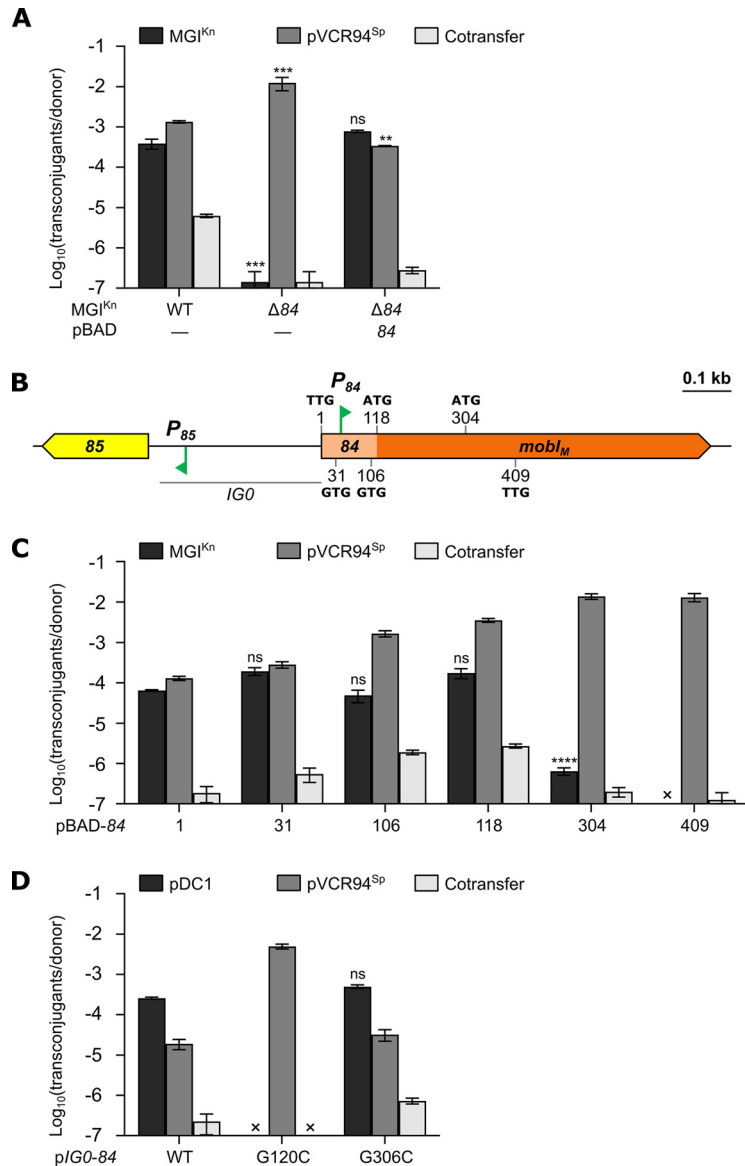


**FIG 2** Role of 84 in MGIVchHai6 mobilization. (A) Mobilization of MGI<sup>Kn</sup> or its  $\Delta 84$  mutant by pVCR94<sup>Sp</sup>. (B) Schematic representation of the 85-84 region of MGIVchHai6. Genes are color coded as indicated in Fig. 1A. The position and sequence of alternative start codons within 84 are indicated. (C) Complementation assays of the  $\Delta 84$  mutation by alternative ORFs within 84. When indicated, donor strains contained the complementation plasmid pBAD-84 or one of its derivatives (Table 1). (D) Confirmation of ATG<sub>118</sub> as the genuine start codon of mobil<sub>M</sub>. Conjugation assays were performed using *E. coli* GG56 (Nx) containing the specified elements as donor strains and either CAG18439 (Tc) (A and C) or VB112 (Rf) (D) as the recipient strain. The bars represent the means  $\pm$  standard errors of the means from three independent experiments. Statistical analyses were carried out on the logarithm of the values using a one-way ANOVA followed by Dunnett's multiple-comparison test with the WT MGI<sup>Kn</sup> (A), pBAD-84 (C), or p/G0-84 (D) as the control. Statistical significance is indicated as follows: \*\*\*\*,  $P < 0.0001$ ; \*\*\*,  $P < 0.001$ ; \*\*,  $P < 0.01$ ; ns, not significant.

and downstream of *trmE*, the integration site of MGIVchHai6, were tested for mobilization. Accordingly, MGI<sup>Cm</sup> or the excision-defective mutant MGI<sup>Cm</sup>  $\Delta xis$  were introduced together with pVCR94<sup>Sp</sup> into *Escherichia coli* BW25113 derivatives carrying a kanamycin resistance (Kn<sup>r</sup>) marker integrated at *uhpC*, *yidX*, *purP*, or *gidB* (Keio knockout collection) (18). These genes are located between 7 and 39.5 kb on either side of *trmE* (Fig. 3C). Mobilization assays failed to produce any transconjugants when the Kn<sup>r</sup> marker was inserted upstream of *trmE*. In contrast, transfer was easily detectable for Kn<sup>r</sup> insertions at *purP* and *gidB* that are located downstream of *trmE*, regardless of the

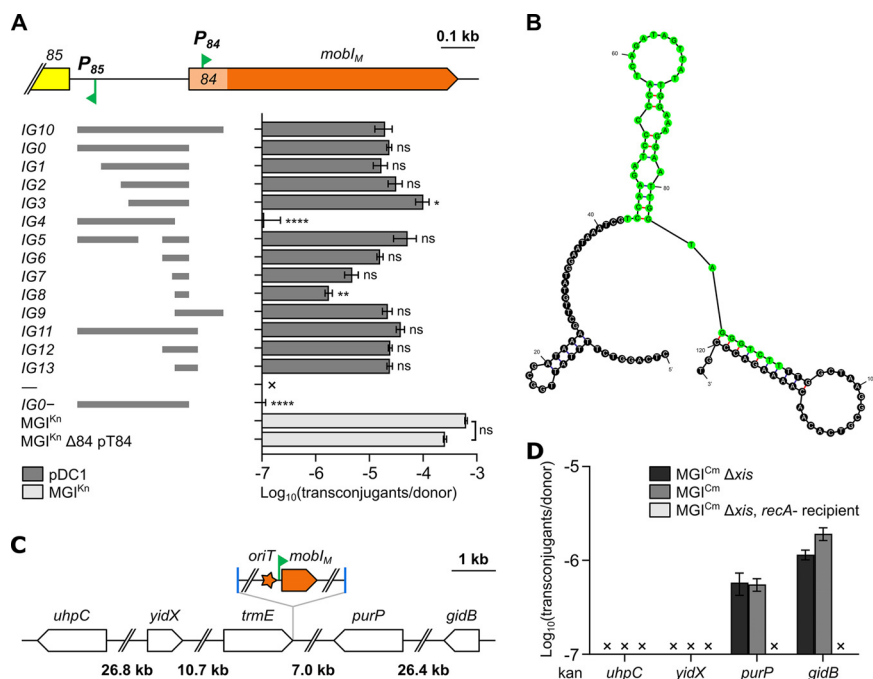


**FIG 3** Localization of the *oriT* locus of MGIVchHai6. (A) On the left, fragments of the 85-*mobI* region that were cloned into the nonmobilizable vector pDC1 are represented by gray bars. The resulting transfer frequencies for the corresponding fragments are presented on the right side. Mobilization assays of pDC1 derivatives were performed using *E. coli* GG56 (Nx) bearing pVCR94<sup>Sp</sup> and pT84 as the donor and VB112 (Rf) as the recipient. “—” indicates an empty pDC1. “IG0—” indicates that the transfer of pIG0 was assessed in the absence of pT84. Statistical analyses were carried out on the logarithm of the values using a one-way ANOVA followed by Dunnett’s multiple-comparison test with pIG10 or MGI<sup>Kn</sup> as the control. Statistical significance is indicated as follows: \*\*\*\*,  $P < 0.0001$ ; \*\*,  $P < 0.01$ ; \*,  $P < 0.05$ ; ns, not significant. (B) Predicted folding of IG12, with IG8 highlighted in green. Folding of the upper strand (panel A) was predicted using the Mfold web server (74). (C) Schematic map of the chromosomal region surrounding *trmE* in *E. coli* K-12. The position and orientation of MGI<sup>Cm</sup> are indicated. (D) MGI<sup>Cm</sup>-mediated mobilization of chromosomal markers from *E. coli* JW3642, JW3692, JW3718, or JW5858 (Kn) bearing pVCR94<sup>Sp</sup> and MGI<sup>Cm</sup> or its  $\Delta$ *xis* mutant to CAG18439 or its  $\Delta$ *recA* mutant (Tc). In panels A and D, the bars represent the means  $\pm$  standard errors of the means from three independent experiments. “x” indicates that the transfer frequency was below the detection limit ( $<10^{-7}$ ).

ability of MGI<sup>Cm</sup> to excise from the chromosome (Fig. 3D). This result demonstrates that transfer of MGIVchHai6 initiated at *oriT* progresses downstream of *mobI<sub>M</sub>* and that the last genes translocated into the recipient cells are *xis-86-85*.

**Involvement of IncC DNA processing genes in MGIVchHai6 mobilization.** To test whether DNA processing genes of IncC plasmids are involved in the mobilization of MGIVchHai6, we constructed nonpolar deletion mutants of *mobI<sub>C</sub>*, *traI*, *traD*, and *traJ* in pVCR94<sup>Sp</sup> and carried out conjugation assays. Each individual deletion abolished transfer of pVCR94<sup>Sp</sup>. Except for *traI*, all deletions could be complemented by ectopic expression of the corresponding gene (Fig. 4A). Complementation of *traI* could not be tested as attempts to clone an intact copy of this gene failed, suggesting that expression under *P<sub>BADr</sub>*, even in the absence of arabinose, is toxic.

As observed for pVCR94<sup>Sp</sup>, deletion of *traI*, *traD*, and *traJ* abolished MGI<sup>Kn</sup> mobilization. Complementation of each mutation restored mobilization to the wild-type level (Fig. 4B). Therefore, these genes appear to be essential for processing and transfer of excised MGI<sup>Kn</sup> DNA. Interestingly, although MGIVchHai6 encodes its own *MobI<sub>M</sub>* factor, deletion of *mobI<sub>C</sub>* resulted in ~100-fold reduction of MGI<sup>Kn</sup> mobilization (Fig. 4B), whereas complementation with pBAD-*mobI<sub>C</sub>* restored mobilization to the wild-type level.

Likewise, we confirmed that MGIVchHai6 relies exclusively on the T4SS encoded by IncC plasmids as deletion of *traH<sub>C</sub>*, *traG<sub>C</sub>*, or *traN<sub>C</sub>* abolished mobilization of MGI<sup>Kn</sup> (Fig. S2). Moreover, mobilization of MGI<sup>Kn</sup> by pVCR94<sup>Sp</sup> into a recipient strain carrying

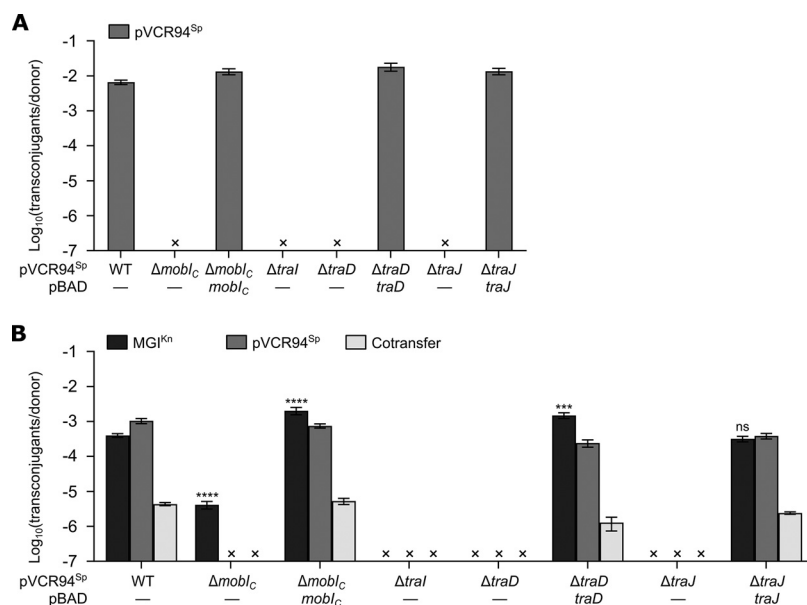
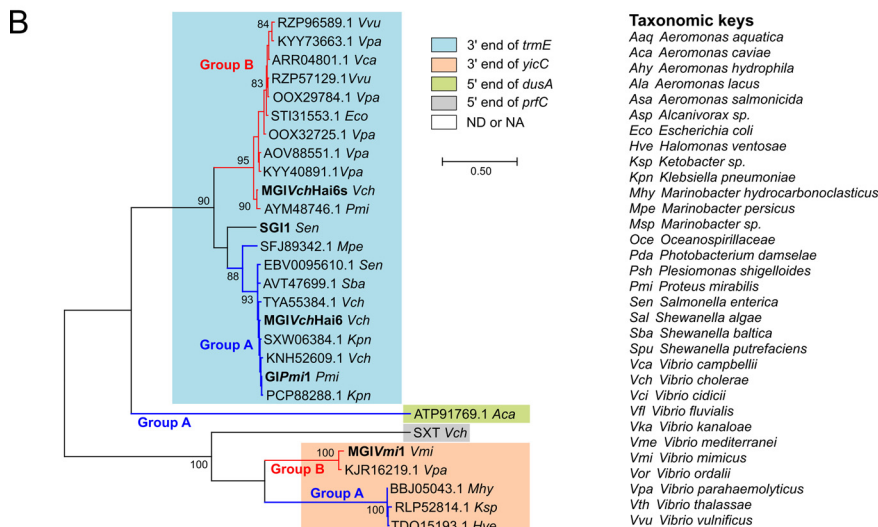
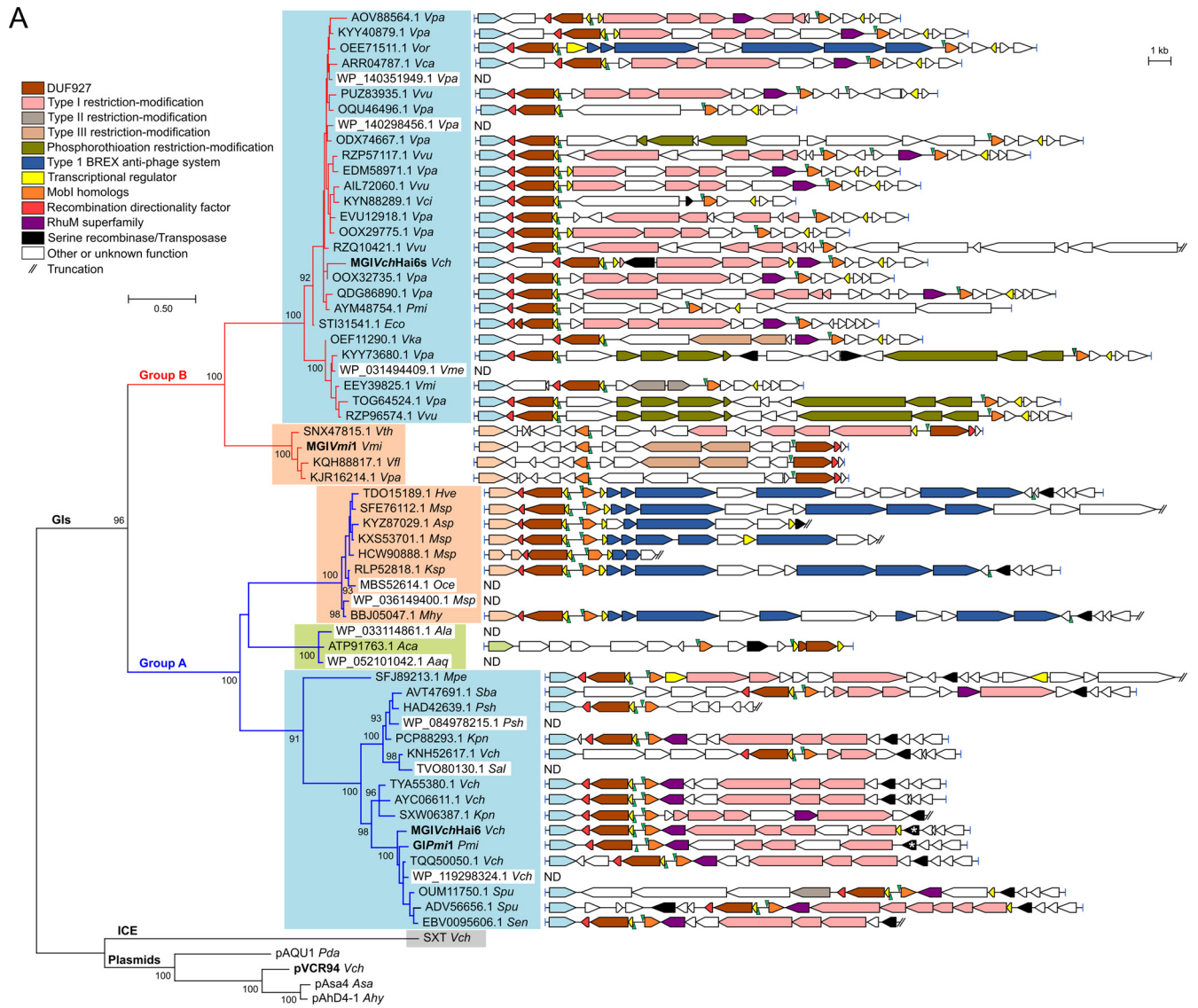


**FIG 4** Mobilization of MGIVchHai6 relies on the T4CP and relaxase encoded by IncC plasmids. (A) Impact of *mobl*<sub>C</sub>, *tral*, *traD*, and *traJ* deletions on pVCR94<sup>Sp</sup> transfer. (B) Mobilization of MGI<sup>Kn</sup> by the *mobl*<sub>C</sub>, *tral*, *traD*, and *traJ* deletion mutants of pVCR94<sup>Sp</sup>. Conjugation assays were performed with *E. coli* GG56 (Nx) containing the specified elements as donor strains and CAG18439 (Tc) as the recipient strain. The bars represent the means ± standard errors of the means from three independent experiments. “x” indicates that the transfer frequency was below the detection limit (<10<sup>-7</sup>). Statistical analyses were carried out on the logarithm of the values using a one-way ANOVA followed by Dunnett’s multiple-comparison test with WT MGI<sup>Kn</sup> as the control. Statistical significance is indicated as follows: \*\*\*\*, *P* < 0.0001; \*\*\*, *P* < 0.001; ns, not significant.

pVCR94<sup>Cm</sup> was abolished (Fig. S2), thus confirming that MGIVchHai6 does not evade IncC entry exclusion.

**MGIVchHai6 is the prototype of a large and diverse subfamily of GIs mobilizable by IncC plasmids.** Given the importance of Mobl-like factors, we searched the GenBank database for Mobl homologs and extracted associated sequences to assess diversity of the GIs related to MGIVchHai6 (see Table S1 in the supplemental material). Phylogenetic analyses of Mobl proteins revealed that Mobl homologs encoded by GIs are distinct from those encoded by conjugative plasmids and cluster in two major groups (Fig. 5A). Group A contains GIs integrated at the 3’ end of *trmE* or *yicC*, and at the 5’ end of *dusA*. With the exception of the GI inserted at *dusA*, all GIs encoding group A Mobl proteins exhibited the same structure: *int-xis-86-85-ig-mobl*, where *ig* likely contains the *oriT*, and *xis-86-85* and *mobl* are divergent and preceded by AcaCD-like binding sites. In a few GIs, variable DNA is inserted between the convergent *int* and *xis* genes. MGIVchHai6 and GIPmi1 belong to group A. GIPmi1 of *Proteus mirabilis* resembles MGIVchHai6, and it contains a large multidrug resistance cluster inserted at the same position but lacks the mercury resistance transposon Tn6310 (19). Most *trmE*-specific group A GIs encode predicted type I restriction-modification (R/M) systems. In contrast, the *yicC*-specific group A GIs encode predicted type 1 BREX antiphage systems.

GIs coding for group B Mobl proteins are integrated either at the 3’ end of *trmE* or 3’ end of *yicC*. In group B GIs, the *xis-86-85* cluster is separated from *mobl* by a large region of variable DNA often encoding predicted type I or phosphorothioation R/M systems. Furthermore, while *trmE*-specific group B GIs conserved the overall structure of group A GIs, *yicC*-specific group B GIs lack 85 and have undergone an inversion of the *xis-86-to-mobl* region relative to the *int* gene. These GIs encode predicted type I and type II R/M systems. Surprisingly, analysis undertaken in this study led to discovery of MGIVchHai6s, a group B GI inserted at *trmE* in a tandem fashion directly downstream of MGIVchHai6 in *V. cholerae* HC-36A1. Unlike MGIVchHai6, MGIVchHai6s does not carry



- Taxonomic keys**
- Aaq* *Aeromonas aquatica*
  - Aca* *Aeromonas caviae*
  - Ahy* *Aeromonas hydrophila*
  - Ala* *Aeromonas lacus*
  - Asa* *Aeromonas salmonicida*
  - Asp* *Alcanivorax* sp.
  - Eco* *Escherichia coli*
  - Hve* *Halomonas ventosae*
  - Ksp* *Ketobacter* sp.
  - Kpn* *Klebsiella pneumoniae*
  - Mhy* *Marinobacter hydrocarbonoclasticus*
  - Mpe* *Marinobacter persicus*
  - Msp* *Marinobacter* sp.
  - Oce* *Oceanospirillaceae*
  - Pda* *Photobacterium damselae*
  - Psh* *Plesiomonas shigelloides*
  - Pmi* *Proteus mirabilis*
  - Sen* *Salmonella enterica*
  - Sal* *Shewanella algae*
  - Sba* *Shewanella baltica*
  - Spu* *Shewanella putrefaciens*
  - Vca* *Vibrio campbellii*
  - Vch* *Vibrio cholerae*
  - Vci* *Vibrio cidei*
  - Vfl* *Vibrio fluvialis*
  - Vka* *Vibrio kanaloae*
  - Vme* *Vibrio mediterranei*
  - Vmi* *Vibrio mimicus*
  - Vor* *Vibrio ordalii*
  - Vpa* *Vibrio parahaemolyticus*
  - Vth* *Vibrio thalassae*
  - Vvu* *Vibrio vulnificus*

**FIG 5** Diversity of genomic islands encoding MobI homologs. (A and B) Maximum likelihood phylogenetic analysis of MobI (A) and Int (B) homologs. Trees with the highest likelihoods (−7,967.92 and −5,688.94 for MobI and Int, respectively) are shown. Bootstrap supports are indicated as percentages at the (Continued on next page)

antibiotic or heavy metal resistance genes. The group B GI of *P. mirabilis* JN40 encoding AYM48754.1 is also integrated in a tandem fashion downstream of SGI1-*Pm*JN40, an SGI1-like element that confers multidrug resistance (20). Thus, tandem integration of different GIs in *trmE* is not a rare occurrence.

Phylogenetic analysis of integrases encoded by respective GIs revealed similar clustering into groups A and B within *trmE*- and *yicC*-specific integrase clusters (Fig. 5B). Although the integrase encoded by SGI1 also mediates integration at *trmE*, it could not be ascribed to either group with confidence (<80 bootstraps), which is consistent with the considerable structural and genetic differences between SGI1-like and MGIV*ch*Hai6-like GIs.

## DISCUSSION

Bacterial conjugation typically results from concerted action of the cytoplasmic relaxosome responsible for DNA processing initiated at *oriT*, and the type IV secretion system (T4SS) that translocates the processed DNA across cell membranes into the recipient cell (21, 22). The type IV coupling protein (T4CP), an inner membrane-anchored protein, acts as a relaxosome docking station at the T4SS. In most cases, the relaxosome comprises a relaxase working together with auxiliary proteins that either help or are required for the relaxase activity. Most of the auxiliary factors hitherto described alter DNA topology by either locally bending DNA at the *oriT* or unwinding DNA through a helicase activity (23–29). Several *oriT*-binding factors, such as TraJ of RP4, TrwA of R388, and Int of Tn916, take part in specific recruitment of the relaxase at this locus (30–34). Other known auxiliary factors are involved in recognition of the T4CP or in relaxosome stabilization by protein-protein interactions (34–36).

Together with SXT/R391 elements, IncC and IncA plasmids share a set of transfer genes encoding a T4SS of the MPF<sub>F</sub> family, a coupling protein (TraD), a relaxase of the MOB<sub>H1</sub> family (Tral), and two essential factors thought to be part of the relaxosome (TraJ [DUF4400, PF14348] and MobI) (8, 10, 11, 37). We have also shown here that TraJ is essential to transfer of IncC plasmids and MGIV*ch*Hai6 (Fig. 4A and B). While results obtained with SXT and the IncHI1 plasmid R27 suggest a role as a relaxosome component (37–39), the exact function of TraJ remains unknown. MobI is required for conjugative transfer of IncC plasmids and SXT/R391 integrative and conjugative elements (ICEs) as well as GIs that mimic the *oriT* locus of the latter but lack a *mobI* gene (10, 40, 41). In contrast, deletion of *mobI* in the helper element does not abolish transfer of pCloDF13 and SGI1, which possess unique *oriT* loci and cognate mobilization proteins MobBC for pCloDF13 and MpsAB for SGI1 (12, 16, 40, 42). MGIV*ch*Hai6 lacks the mobilization genes *mpsAB* and the *oriT* locus that are essential for SGI1 mobilization (13, 16). Instead, we showed that MGIV*ch*Hai6 encodes MobI<sub>M</sub>, a distant homolog of the IncC plasmid-encoded MobI<sub>C</sub> that provides some independence from *mobI<sub>C</sub>* (Fig. 1A, 2A, and 4B). Deletion of *mobI<sub>C</sub>* in the IncC plasmid R16a was shown to enhance (45-fold increase) mobilization of SGI1-C, suggesting competition between SGI1-C and its helper plasmid for the conjugative machinery (12). In contrast, we found that the absence of *mobI<sub>C</sub>* impaired transfer of MGIV*ch*Hai6 (~100-fold decrease) (Fig. 4B), suggesting that MobI<sub>C</sub> enhances initiation of transfer mediated by Tral and MobI<sub>M</sub> at *oriT* of MGIV*ch*Hai6. However, deletion of *mobI<sub>M</sub>*, while abolishing MGIV*ch*Hai6 mobilization, also enhanced transfer of the helper plasmid (12-fold increase) (Fig. 2A), consistent with competition between the two elements.

We identified the *oriT* locus of MGIV*ch*Hai6 within the intergenic region upstream of

### FIG 5 Legend (Continued)

branching points only when >80%. Branch lengths represent the number of substitutions per site over 201 and 311 amino acid positions for MobI and Int, respectively. Only one representative per cluster of similar proteins (>95% identity threshold) is shown in each tree. In panel A, the schematic structure of the genomic island encoding the corresponding MobI protein is shown next to each node. ORFs with similar function are color coded as indicated in the panel. Each node and the integrase gene of the corresponding node are color coded based on the integration site of the genomic island (refer to panel B for color key [ND, not determined; NA, not available]). Vertical green arrowheads indicate position and orientation of AcaCD binding sites. *attL* and *attR* attachment sites flanking each GI are represented by blue bars. The asterisks in MGIV*ch*Hai6 and GI*Pmi*1 indicate the insertion site of the complex resistance integrons. Additional details on GIs and host strains are provided in Table S1 in the supplemental material.

*mobl<sub>M</sub>* (*IG0*) and found that a 49-bp region (*IG8*) was sufficient to promote mobilization of a nonmobilizable plasmid. While *IG0* shares low nucleotide identity (45%) with the *oriT* of pVCR94 (10, 12), the 49-bp *IG8* shares 63% identity with this *oriT*, with the last 32 bp of *IG8* sharing 84% with the corresponding region in pVCR94 *oriT*. Nevertheless, this level of conservation is notably limited compared to the similarity reported between *oriT* of SXT and the GIs it mobilizes (>63% over ~300 bp) (41). This lack of conservation likely accounts for the requirement for *Mobl<sub>M</sub>* to achieve optimal transfer of MGIVchHai6. Together with the absence of a *Mobl* homolog in SXT-mobilizable GIs, the specificity of *Mobl<sub>M</sub>* and *Mobl<sub>C</sub>* for their respective elements further supports the proposed role for *Mobl* as an auxiliary relaxosome component involved in *oriT* recognition (40, 43).

SGI1 encodes three functional T4SS subunits, TraH<sub>S</sub>, TraG<sub>S</sub>, and TraN<sub>S</sub>, that displace the homologous subunits encoded by IncC plasmids despite strong amino acid sequence divergences (64, 37, and 78% identity, respectively) (17). This alteration of the mating channel is crucial to enhance SGI1 mobilization (13, 17). Incorporation of TraG<sub>S</sub> into the IncC mating pore allows SGI1 to circumvent entry exclusion exerted by an IncC plasmid in the recipient cells, allowing SGI1 to spread freely, even in a population of cells carrying IncC plasmids (17, 44). In contrast, MGIVchHai6 lacks genes encoding T4SS subunits. Predictably, MGIVchHai6 was shown here to conform to IncC entry exclusion and thus is unable to transfer to a strain already containing an IncC plasmid (see Fig. S2 in the supplemental material).

In SGI1, AcaCD binding sites have been identified upstream of *xis*, *S004-rep*, *traN<sub>S</sub>*, *traHG<sub>S</sub>*, and *S018* and corresponding promoters shown to respond to AcaCD activation (9, 17, 45–47). In MGIVchHai6, putative AcaCD binding sites were predicted at the 5' end of *84* and upstream of an operon-like gene cluster containing *xis*, which encodes a putative protein sharing only 37% identity with the RDF Xis of SGI1 (13). In this study, Xis is indeed an RDF acting together with Int to catalyze excision under the control of AcaCD (Fig. 1B and C and Fig. S1). Regulation of *xis* and *mobl* by AcaCD is consistent with the previously proposed model in which these GIs remain quiescent in the chromosome in the absence of an IncC plasmid (43).

MGIVchHai6-like elements have been detected *in silico* in environmental and clinical O1 and non-O1/non-O139 *V. cholerae* isolates from the Indian subcontinent and South America, and in *Shewanella* sp. from North America, although those seem to be devoid of antibiotic resistance genes (13). IDH-03944, a cotrimoxazole resistance-conferring GI related to MGIVchHai6, was recently reported in a 2011 isolate of *V. cholerae* O44 recovered from diarrheal patients in Kolkata, India (48). Comparative genomics revealed a much more diverse set of GIs related to MGIVchHai6 in the genome of marine dwelling species and integrated at the 3' end of *trmE* and *yicC* or at the 5' end of *dusA* (Fig. 5). The gene cargo of these GIs is predominantly associated with DNA modification (methylation, phosphorothioation) and restriction systems, as well as antiphage systems such as BREX (Fig. 5A). Only MGIVchHai6 and GIPmi1, together with IDH-03944 (48), contained integrons carrying antibiotic resistance genes, suggesting that these elements are an ancient, large reservoir of antiphage systems, recently hijacked as vectors for drug resistance genes. Most GIs of the MGIVchHai6 and MGIVchHai6s clades share a gene encoding a predicted RhuM-like virulence factor, usually immediately upstream or downstream of *mobl<sub>M</sub>* (Fig. 5). A mutant of *rhuM* located in *S. enterica* SPI-3 pathogenicity island is deficient for epithelial cell invasion, neutrophil transmigration, and killing of its *Caenorhabditis elegans* host (49). While these results suggest that MGIVchHai6-like elements may be involved in virulence modulation, the molecular function of RhuM is not known and its potency in the *Vibrionaceae* has not been assessed. One striking feature of MGIVchHai6-like elements is the syntenic conservation of an operon-like region typically including a predicted AcaCD binding site followed by genes encoding a putative transcriptional regulator containing a helix-turn-helix (HTH) domain, a DUF927 domain-containing protein, and the *xis* gene (Fig. 5A). While the DUF927 gene is ubiquitous, GIs of the MGIVmi1 clade lack the upstream transcriptional regulator gene and the AcaCD binding site is located directly upstream of the DUF927

gene. Such high conservation is even more surprising since 85 and 86 are dispensable for mobilization of MGIVchHai6 by its helper plasmid (Fig. 1B). Why such factors should be under the control of the IncC transfer activator AcaCD is puzzling. Interestingly, a similar region exists in GIs mobilized by ICEs of the SXT/R391 family (Fig. S3). In prototypical MGIVflnd1, a binding site of the transfer activator SetCD lies upstream of *rdfM* and *cds8*, which encode a predicted transcriptional regulator and a DUF927 domain-encoding protein. While the role of *cds8* remains elusive, RdfM shares weak amino acid identity (25%) with the product of 85 and acts as an RDF, facilitating excision of MGIVflnd1 upon *setCD* expression (50). In addition to the aforementioned factors, MGIVflnd1 and several MGIVchHai6-like GIs share an integration site at the 3' end of *yicC* (Fig. 5B), an observation that prompted us to hypothesize that Xis and 85/RdfM act as alternative RDFs, each allowing excision from a specific integration site. To test this, a  $\Delta$ *rdfM* mutant of MGIVflnd1 was complemented by overexpressing 85 in a strain also containing ICEVflnd1 to provide *setCD*. However, 85 failed to restore excision and an *attP* or *attB* junction was not detected (data not shown), suggesting that 85 has a different function or is too divergent to promote excision of MGIVflnd1.

SXT/R391 ICEs have been shown to promote conjugative transfer of chromosomal DNA located 3' of *prfC*, their integration site, and remotely 5' of *yicC*, the integration site of the GIs they mobilize (41, 51). Thus, these elements are able to mobilize large stretches ( $\geq 1$ Mbp) of chromosomal DNA locally and remotely in an Hfr-like manner, suggesting that SXT/R391 ICEs play an evolutionary role that extends beyond their own dissemination. Our results show that IncC plasmids can mobilize chromosomal DNA located downstream of *trmE* by mobilization of MGIs without their prior excision from the chromosome (Fig. 3). Given the presence of MGIVchHai6-like elements integrated at different chromosomal sites and across a wide range of *Vibrionaceae* and other species of *Gammaproteobacteria*, IncC plasmids and their subordinate GIs can be concluded to comprise a potent driving force in the gene flow circulating in many bacterial pathogens. In fact, this is superbly exemplified by the recently reported presence of an MGIVchHai6-like GI in *V. cholerae* Santiago-089, a non-O1/non-O139 clinical isolate harboring many virulence genes scattered throughout chromosome 1 (52). Not only is the GI itself poised to be mobilized by an incoming IncC plasmid—along with the GI-borne antibiotic and mercury resistance genes—but it is also plausible that it may, in fact, usher transfer of downstream elements GIVch-T3SS and VPI-2, thus simultaneously contributing to dissemination of virulence determinants.

Cholera continues to cause epidemics that include millions of cases worldwide (53). The geographical range of *V. cholerae* is expected to expand dramatically as climate change renders the marine environment increasingly hospitable to this pathogen (54, 55). While the ability to promote epidemic outbreaks was traditionally regarded as an appanage of O1 and O139 strains (56), it is becoming increasingly clear that the actual picture is far more nuanced (52, 57–60). In various species, cumulative acquisition of antibiotic resistance and/or virulence determinants through exchange of genomic islands has time and again allowed emergence of virulent strains, some of which lack canonical virulence hallmarks (61–63). IncC plasmids circulating in non-O1/non-O139 *V. cholerae* populations may prove to comprise the perfect trigger for emergence of unforeseen pandemics.

## MATERIALS AND METHODS

**Bacterial strains and media.** The bacterial strains and plasmids used in this study are described in Table 1. The strains were routinely grown in lysogeny broth (LB) (EMD) at 37°C in an orbital shaker and stored at –80°C in LB broth with 15% (vol/vol) glycerol. The following antibiotics and concentrations were employed: ampicillin (Ap), 50  $\mu$ g/ml; chloramphenicol (Cm), 20  $\mu$ g/ml; kanamycin (Kn), 10  $\mu$ g/ml for single-copy integrants of pOPlacZ-derived constructs, 50  $\mu$ g/ml otherwise; nalidixic acid (Nx), 40  $\mu$ g/ml; rifampin (Rf), 50  $\mu$ g/ml; spectinomycin (Sp), 50  $\mu$ g/ml; streptomycin (Sm), 200  $\mu$ g/ml; tetracycline (Tc), 12  $\mu$ g/ml. Conjugation assays were performed as previously described (17). However, donors and recipients were selected according to their sole chromosomal markers. When required, mating experiments were performed using LB plates with 0.02% arabinose to induce expression of pBAD30-derived

**TABLE 1** Strains and plasmids used in this study

Strain, plasmid, or element	Relevant genotype or phenotype <sup>a</sup>	Reference
<i>Vibrio cholerae</i> HC-36A1	Clinical, non-O1/non-O139, Haiti, 2010 (Ap Cm Kn Sp Sm Su Tc Tm)	57
<i>Escherichia coli</i>		
BW25113	F <sup>-</sup> $\Delta(\text{araD-araB})567 \Delta\text{lacZ4787}::\text{rrnB-3} \lambda^- \text{rph-1} \Delta(\text{rhaD-rhaB})568 \text{hsdR514}$	75
GG56	Nx <sup>r</sup> derivative of BW25113 (Nx)	76
VB112	Rf <sup>r</sup> derivative of MG1655 (Rf)	40
CAG18439	MG1655 <i>lacZU118 lacI42::Tn10</i> (Tc)	77
VB47	CAG18439 $\Delta\text{recA} \Delta\text{galK}$	78
JW3642	BW25113 $\Delta\text{uhpC772}::\text{aph}$ (Kn)	18
JW3692	BW25113 $\Delta\text{purP745}::\text{aph}$ (Kn)	18
JW3718	BW25113 $\Delta\text{gidB769}::\text{aph}$ (Kn)	18
JW5858	BW25113 $\Delta\text{yidX732}::\text{aph}$ (Kn)	18
Plasmids		
pVCR94	IncC conjugative plasmid, <i>V. cholerae</i> O1 El Tor (Su Tm Cm Ap Tc Sm)	10
pVCR94 <sup>Sp</sup>	Sp <sup>r</sup> derivative of pVCR94 (pVCR94 $\Delta$ X2) (Su Sp)	9
pVCR94 <sup>Kn</sup>	Kn <sup>r</sup> derivative of pVCR94 (pVCR94 $\Delta$ X3) (Su Kn)	9
pVCR94 <sup>Cm</sup>	Cm <sup>r</sup> derivative of pVCR94 (pVCR94 $\Delta$ X4) (Su Cm)	17
pVCR94 $\Delta$ <i>mobl</i> <sub>C</sub>	<i>mobl</i> <sub>C</sub> deletion mutant of pVCR94 <sup>Sp</sup> (Su Sp)	This study
pVCR94 $\Delta$ <i>tral</i>	<i>tral</i> deletion mutant of pVCR94 <sup>Sp</sup> (Su Sp)	This study
pVCR94 $\Delta$ <i>traD</i>	<i>traD</i> deletion mutant of pVCR94 <sup>Sp</sup> (Su Sp)	This study
pVCR94 $\Delta$ <i>traJ</i>	<i>traJ</i> deletion mutant of pVCR94 <sup>Sp</sup> (Su Sp)	This study
pVCR94 $\Delta$ <i>traN</i>	<i>traN</i> deletion mutant of pVCR94 <sup>Sp</sup> (Su Sp)	9
pVCR94 $\Delta$ <i>traG</i>	<i>traG</i> deletion mutant of pVCR94 <sup>Sp</sup> (Su Sp)	9
pVCR94 $\Delta$ <i>traH</i>	<i>traH</i> deletion mutant of pVCR94 <sup>Sp</sup> (Su Sp)	9
pBAD30	<i>ori</i> <sub>p15A</sub> <i>bla</i> <i>araC</i> <i>P</i> <sub>BAD</sub> (Ap)	79
<i>pacaCD</i>	pBAD30:: <i>acaDC</i> (Ap)	9
pBAD- <i>mobl</i> <sub>C</sub>	pBAD30:: <i>mobl</i> <sub>C</sub> (Ap)	This study
pBAD- <i>traD</i>	pBAD30:: <i>traD</i> (Ap)	This study
pBAD- <i>traJ</i>	pBAD30:: <i>traJ</i> (Ap)	This study
pBAD- <i>traN</i>	pBAD30:: <i>traN</i> (Ap)	17
pBAD- <i>traG</i>	pBAD30:: <i>traG</i> (Ap)	17
pBAD- <i>traH</i>	pBAD30:: <i>traH</i> (Ap)	17
pBAD- <i>int</i>	pBAD30:: <i>int</i> (Ap)	This study
pBAD- <i>xis</i>	pBAD30:: <i>xis</i> (Ap)	This study
pT84	pBAD-TOPO:: <i>84</i> (Ap)	This study
pBAD-84	pBAD30:: <i>84</i> (Ap)	This study
pBAD-84-31	pBAD30:: <i>84</i> starting at position +31 of <i>84</i> (Ap)	This study
pBAD-84-106	pBAD30:: <i>84</i> starting at position +106 of <i>84</i> (Ap)	This study
pBAD-84-118	pBAD30:: <i>84</i> starting at position +118 of <i>84</i> (Ap)	This study
pBAD-84-304	pBAD30:: <i>84</i> starting at position +304 of <i>84</i> (Ap)	This study
pBAD-84-409	pBAD30:: <i>84</i> starting at position +409 of <i>84</i> (Ap)	This study
pOPlacZ	<i>ori</i> <sub>r6K<math>\gamma</math></sub> <i>attP</i> <sub><math>\lambda</math></sub> <i>aph lacZ</i> (Kn)	9
pPromint	pOPlacZ containing -163 to -12 of MGIVchHai6 <i>P</i> <sub>int</sub> (Kn)	This study
pProm85	pOPlacZ containing -389 to -11 of MGIVchHai6 <i>P</i> <sub>85</sub> (Kn)	This study
pProm <i>mobl</i>	pOPlacZ containing -345 to -11 of MGIVchHai6 <i>P</i> <sub>84</sub> (Kn)	This study
pProm <i>traH</i> <sub>5</sub>	pOPlacZ containing -243 to -14 of SGI1 <i>P</i> <sub>traH5</sub> (Kn)	17
pDC1	pACYC184 $\Delta\text{cat}$ ( $\Delta$ MscI-PvuII) (Tc)	40
pIG0-84	pDC1:: <i>IG0-84</i> (Tc)	This study
pIG0-84G120C	pDC1:: <i>IG0-84</i> G120C (Tc)	This study
pIG0-84G306C	pDC1:: <i>IG0-84</i> G306C (Tc)	This study
pIG0	pDC1:: <i>IG0</i> (Tc)	This study
pIG1	pDC1:: <i>IG1</i> (Tc)	This study
pIG2	pDC1:: <i>IG2</i> (Tc)	This study
pIG3	pDC1:: <i>IG3</i> (Tc)	This study
pIG4	pDC1:: <i>IG4</i> (Tc)	This study
pIG5	pDC1:: <i>IG5</i> (Tc)	This study
pIG6	pDC1:: <i>IG6</i> (Tc)	This study
pIG7	pDC1:: <i>IG7</i> (Tc)	This study
pIG8	pDC1:: <i>IG8</i> (Tc)	This study
pIG9	pDC1:: <i>IG9</i> (Tc)	This study
pIG10	pDC1:: <i>IG10</i> (Tc)	This study
pIG11	pDC1:: <i>IG11</i> (Tc)	This study
pIG12	pDC1:: <i>IG12</i> (Tc)	This study

(Continued on next page)

TABLE 1 (Continued)

Strain, plasmid, or element	Relevant genotype or phenotype <sup>a</sup>	Reference
p <i>G13</i>	pDC1::iG13 (Tc)	This study
pINT-ts	<i>oriR101 cl857 λP<sub>R</sub>-int<sub>λ</sub></i> (ts, Ap)	80
pSIM6	λRed recombination thermo-inducible encoding plasmid (ts, Ap)	81
pMS1	λRed recombination thermo-inducible encoding plasmid (ts, Gm)	10
pKD3	<i>cat</i> (Cm) template for one-step chromosomal gene inactivation	75
pKD4	<i>aph</i> (Kn) template for one-step chromosomal gene inactivation	75
pCP20	Flp recombinase thermo-inducible encoding plasmid (ts, Ap Cm)	82
pCP20-Gm	Gm <sup>r</sup> derivative of pCP20 (ts, Gm Cm)	83
Genomic islands		
MGI <i>Vch</i> Hai6	Drug resistance island, <i>V. cholerae</i> HC-36A1 (Ap Cm Sm Su Tm Tc)	13
MGI <sup>Kn</sup>	Kn <sup>r</sup> derivative of MGI <i>Vch</i> Hai6 lacking In36A1 and Tn6310 (Kn)	This study
MGI <sup>Cm</sup>	Cm <sup>r</sup> derivative of MGI <i>Vch</i> Hai6 lacking In36A1 and Tn6310 (Cm)	This study
MGI <sup>Kn</sup> Δ <i>int</i>	<i>int</i> deletion mutant of MGI <sup>Kn</sup> (Kn)	This study
MGI <sup>Kn</sup> Δ <i>xis</i>	<i>xis</i> deletion mutant of MGI <sup>Kn</sup> (Kn)	This study
MGI <sup>Cm</sup> Δ <i>xis</i>	<i>xis</i> deletion mutant of MGI <sup>Cm</sup> (Cm)	This study
MGI <sup>Kn</sup> Δ86	86 deletion mutant of MGI <sup>Kn</sup> (Kn)	This study
MGI <sup>Kn</sup> Δ85	85 deletion mutant of MGI <sup>Kn</sup> (Kn)	This study
MGI <sup>Kn</sup> Δ84	84 deletion mutant of MGI <sup>Kn</sup> (Kn)	This study

<sup>a</sup>Ap, ampicillin; Cm, chloramphenicol; Gm, gentamicin; Kn, kanamycin; Nx, nalidixic acid; Rf, rifampin; Sp, spectinomycin; Sm, streptomycin; Su, sulfamethoxazole; Tc, tetracycline; Tm, trimethoprim; ts, thermosensitive.

complementation vectors. The frequencies of transconjugant formation were computed as ratios of transconjugant per donor CFU from three independent mating experiments.

**Molecular biology methods.** Plasmid DNA was extracted using the EZ-10 Spin Column Plasmid DNA Minipreps kit (Bio Basic) following the manufacturer's instructions. Enzymes used in this study were purchased from New England Biolabs. PCR assays were performed with the primers listed in Table 2. PCR conditions were as follows: (i) 3 min at 94°C; (ii) 30 cycles, with 1 cycle consisting of 30 s at 94°C, 30 s at the appropriate annealing temperature, and 1 min/kb at 68°C; and (iii) 5 min at 68°C. When required, the resulting products were purified using the EZ-10 Spin Column PCR Products purification kit (Bio Basic) following the manufacturer's instructions. *E. coli* strains were transformed by electroporation as described previously (64) in a Bio-Rad Gene Pulser Xcell device set at 25 μF, 200 V, and 1.8 kV using 1-mm gap electroporation cuvettes.

**Plasmid and strain construction.** The plasmids and primers used in this study are listed in Tables 1 and 2, respectively. Detailed description of plasmid and strain construction is provided in Text S1 in the supplemental material.

**Detection of MGI*Vch*Hai6 excision.** Excision of MGI*Vch*Hai6 was detected by PCR on genomic DNA of the appropriate strains using primers listed in Table 2. The *attR* and *attP* sites were respectively amplified using primer pairs 43\_attPF/Ec104D.rev and 43\_attPF/Hai6\_attPR.

**β-Galactosidase assays.** Qualitative assays were performed by depositing 10-μl aliquots of overnight cultures with appropriate antibiotics on solid agar supplemented with 5-bromo-4-chloro-3-indolyl-β-D-galactopyranoside (X-gal) with or without 0.02% arabinose. The plates were observed after an overnight incubation at 37°C.

Quantitative assays were performed with 2-nitrophenyl-β-D-galactopyranoside (ONPG) according to a protocol adapted from Miller (65). After an overnight incubation at 37°C with appropriate antibiotics, cultures were diluted 1:100 in 50 ml LB broth supplemented with 50 μg/ml ampicillin and grown until an optical density at 600 nm (OD<sub>600</sub>) of 0.2 was reached. Two series of 1/10 dilutions were then prepared in total volumes of 5 ml LB broth supplemented with 50 μg/ml ampicillin with or without 0.2% arabinose and incubated for 2 h at 37°C.

**Phylogenetic analyses.** The primary sequence of homologs of MobI proteins encoded by MGI*Vch*-Hai6 and MGI*Vmi*1 were obtained using the NCBI blastp algorithm (66) against the nr/nt database restricted to *Gammaproteobacteria* (taxid: 1236). Primary sequences sharing less than 45% identity and under 85% minimum coverage were filtered out of subsequent analyses. Distant MobI homologs from SXT (GenBank accession no. EET25017.1), pVCR94 (GenBank WP\_001447712.1), pAhD4-1 (GenBank ALZ82609.1), pAsa4 (GenBank ABO92354.1), and pAQU1 (GenBank WP\_014386842.1) were introduced manually in the data set as an outgroup. MobI homologs were first clustered with CD-HIT (67) to the best cluster that met the 0.95 identity cutoff prior to alignment. The predicted primary sequences of Int homologs were recovered from a representative sample of GIs encoding MobI homologs. Int primary sequences of SXT and SGI1 (GenBank accession no. AF261825.2) were introduced manually. Phylogenetic analyses were computed using amino acid alignments generated by MUSCLE (68). Prior to phylogenetic analysis, poorly aligned regions were discarded using trimAl v1.3 software with the automated heuristic approach (69). Evolutionary analyses were performed within MEGA X (v 10.0.5) (70) using the maximum likelihood method (PhyML) (71) and either the JTT (MobI) or LG (Int) matrix-based models (72, 73). The initial tree(s) for the heuristic search was obtained automatically by applying neighbor-joining and BioNJ algorithms to a matrix of pairwise distances estimated using a JTT model and then selecting the topology with superior log likelihood value.



TABLE 2 (Continued)

Primer name	Nucleotide sequence (5' to 3') <sup>a</sup>	Reference
minoriT9Xbal.R	NNNN <u>CTAGAG</u> ACATAATCCACTGTATGTTG	This study
minoriT11.R	ACGGGTCTTTTGTGTGAC	This study
Hai6delWEcm.for	TGCCGTAATCAAGGAAATGATACGGCAGAAAGTCGTGGAATACCTGTGACGGAAGATCAC	This study
Hai6delWEcm.rev	TGATTACGACTACCGAAACCATAATTGGGTTTAATGACTGATAGGAACCTTCATTTAAATGG	This study

<sup>a</sup>Restriction sites are underlined.

## SUPPLEMENTAL MATERIAL

Supplemental material is available online only.

**TEXT S1**, DOCX file, 0.02 MB.

**FIG S1**, PDF file, 0.1 MB.

**FIG S2**, PDF file, 0.04 MB.

**FIG S3**, PDF file, 0.1 MB.

**TABLE S1**, XLSX file, 0.03 MB.

## ACKNOWLEDGMENTS

We are grateful to Maude Chabot for technical assistance and members of the Burrus laboratory for insightful discussions.

This work was supported by Discovery Grant (2016-04365) from the Natural Sciences and Engineering Council of Canada (NSERC) and project grant (PJT-153071) from the Canadian Institutes of Health Research (CIHR) to V.B., and FRQS MSc scholarship and Alexander Graham Bell Canada Graduate Scholarship from the NSERC to N.R.

The funders had no role in study design, data collection and interpretation, or the decision to submit the work for publication.

## REFERENCES

- Harris JB, LaRocque RC, Qadri F, Ryan ET, Calderwood SB. 2012. Cholera. *Lancet* 379:2466–2476. [https://doi.org/10.1016/S0140-6736\(12\)60436-X](https://doi.org/10.1016/S0140-6736(12)60436-X).
- Das B, Verma J, Kumar P, Ghosh A, Ramamurthy T. 2020. Antibiotic resistance in *Vibrio cholerae*: understanding the ecology of resistance genes and mechanisms. *Vaccine* 38(Suppl 1):A83–A92. <https://doi.org/10.1016/j.vaccine.2019.06.031>.
- Verma J, Bag S, Saha B, Kumar P, Ghosh TS, Dayal M, Senapati T, Mehra S, Dey P, Desigamani A, Kumar D, Rana P, Kumar B, Maiti TK, Sharma NC, Bhadra RK, Mutreja A, Nair GB, Ramamurthy T, Das B. 2019. Genomic plasticity associated with antimicrobial resistance in *Vibrio cholerae*. *Proc Natl Acad Sci U S A* 116:6226–6231. <https://doi.org/10.1073/pnas.1900141116>.
- Weill F-X, Domman D, Njamkepo E, Tarr C, Rauzier J, Fawal N, Keddy KH, Salje H, Moore S, Mukhopadhyay AK, Bercion R, Luquero FJ, Ngandjio A, Dosso M, Monakhova E, Garin B, Bouchier C, Pazzani C, Mutreja A, Grunow R, Sidikou F, Bonte L, Breurec S, Damian M, Njanpop-Lafourcade B-M, Sapriel G, Page A-L, Hamze M, Henkens M, Chowdhury G, Mengel M, Koeck J-L, Fournier J-M, Dougan G, Grimont PAD, Parkhill J, Holt KE, Piarroux R, Ramamurthy T, Quilici M-L, Thomson NR. 2017. Genomic history of the seventh pandemic of cholera in Africa. *Science* 358:785–789. <https://doi.org/10.1126/science.aad5901>.
- Spagnoletti M, Ceccarelli D, Rieux A, Fondi M, Taviani E, Fani R, Colombo MM, Colwell RR, Balloux F. 2014. Acquisition and evolution of SXT-R391 integrative conjugative elements in the seventh-pandemic *Vibrio cholerae* lineage. *mBio* 5:e01356-14. [CrossRef] <https://doi.org/10.1128/mBio.01356-14>.
- Folster JP, Katz L, McCullough A, Parsons MB, Knipe K, Sammons SA, Boncy J, Tarr CL, Whichard JM. 2014. Multidrug-resistant IncA/C plasmid in *Vibrio cholerae* from Haiti. *Emerg Infect Dis* 20:1951–1953. <https://doi.org/10.3201/eid2011.140889>.
- Wang R, Yu D, Zhu L, Li J, Yue J, Kan B. 2015. IncA/C plasmids harboured in serious multidrug-resistant *Vibrio cholerae* serogroup O139 strains in China. *Int J Antimicrob Agents* 45:249–254. <https://doi.org/10.1016/j.ijantimicag.2014.10.021>.
- Harmer CJ, Hall RM. 2015. The A to Z of A/C plasmids. *Plasmid* 80:63–82. <https://doi.org/10.1016/j.plasmid.2015.04.003>.
- Carraro N, Matteau D, Luo P, Rodrigue S, Burrus V. 2014. The master activator of IncA/C conjugative plasmids stimulates genomic islands and multidrug resistance dissemination. *PLoS Genet* 10:e1004714. <https://doi.org/10.1371/journal.pgen.1004714>.
- Carraro N, Sauv  M, Matteau D, Lauzon G, Rodrigue S, Burrus V. 2014. Development of pVCR94ΔX from *Vibrio cholerae*, a prototype for studying multidrug resistant IncA/C conjugative plasmids. *Front Microbiol* 5:44. <https://doi.org/10.3389/fmicb.2014.00044>.
- Garcill n-Barcia MP, Francia MV, de la Cruz F. 2009. The diversity of conjugative relaxases and its application in plasmid classification. *FEMS Microbiol Rev* 33:657–687. <https://doi.org/10.1111/j.1574-6976.2009.00168.x>.
- Hegy  A, Szab  M, Olasz F, Kiss J. 2017. Identification of *oriT* and a recombination hot spot in the IncA/C plasmid backbone. *Sci Rep* 7:10595. <https://doi.org/10.1038/s41598-017-11097-0>.
- Carraro N, Rivard N, Ceccarelli D, Colwell RR, Burrus V. 2016. IncA/C conjugative plasmids mobilize a new family of multidrug resistance islands in clinical *Vibrio cholerae* non-O1/non-O139 isolates from Haiti. *mBio* 7:e00509-16. <https://doi.org/10.1128/mBio.00509-16>.
- Boyd D, Peters GA, Cloeckert A, Boumedine KS, Chaslus-Dancla E, Imberechts H, Mulvey MR. 2001. Complete nucleotide sequence of a 43-kilobase genomic island associated with the multidrug resistance region of *Salmonella enterica* serovar Typhimurium DT104 and its identification in phage type DT120 and serovar Agona. *J Bacteriol* 183:5725–5732. <https://doi.org/10.1128/JB.183.19.5725-5732.2001>.
- Doublet B, Boyd D, Mulvey MR, Cloeckert A. 2005. The *Salmonella* genomic island 1 is an integrative mobilizable element. *Mol Microbiol* 55:1911–1924. <https://doi.org/10.1111/j.1365-2958.2005.04520.x>.
- Kiss J, Szab  M, Hegy  A, Douard G, Praud K, Nagy I, Olasz F, Cloeckert A, Doublet B. 2019. Identification and characterization of *oriT* and two mobilization genes required for conjugative transfer of *Salmonella* genomic island 1. *Front Microbiol* 10:457. <https://doi.org/10.3389/fmicb.2019.00457>.
- Carraro N, Durand R, Rivard N, Anquetil C, Barrette C, Humbert M, Burrus V. 2017. *Salmonella* genomic island 1 (SGI1) reshapes the mating apparatus of IncC conjugative plasmids to promote self-propagation. *PLoS Genet* 13:e1006705. <https://doi.org/10.1371/journal.pgen.1006705>.
- Baba T, Ara T, Hasegawa M, Takai Y, Okumura Y, Baba M, Datsenko KA, Tomita M, Wanner BL, Mori H. 2006. Construction of *Escherichia coli* K-12

- in-frame, single-gene knockout mutants: the Keio collection. *Mol Syst Biol* 2:2006.0008. <https://doi.org/10.1038/msb4100050>.
19. Siebor E, de Curraize C, Neuwirth C. 2018. Genomic context of resistance genes within a French clinical MDR *Proteus mirabilis*: identification of the novel genomic resistance island *GIPmi1*. *J Antimicrob Chemother* 73: 1808–1811. <https://doi.org/10.1093/jac/dky126>.
  20. Bie L, Fang M, Li Z, Wang M, Xu H. 2018. Identification and characterization of new resistance-conferring SGI1s (*Salmonella* genomic island 1) in *Proteus mirabilis*. *Front Microbiol* 9:3172. <https://doi.org/10.3389/fmicb.2018.03172>.
  21. Llosa M, Gomis-Rüth FX, Coll M, de la Cruz Fd F. 2002. Bacterial conjugation: a two-step mechanism for DNA transport. *Mol Microbiol* 45:1–8. <https://doi.org/10.1046/j.1365-2958.2002.03014.x>.
  22. Ilangovan A, Connery S, Waksman G. 2015. Structural biology of the Gram-negative bacterial conjugation systems. *Trends Microbiol* 23: 301–310. <https://doi.org/10.1016/j.tim.2015.02.012>.
  23. Luo Y, Gao Q, Deonier RC. 1994. Mutational and physical analysis of F plasmid TraY protein binding to *oriT*. *Mol Microbiol* 11:459–469. <https://doi.org/10.1111/j.1365-2958.1994.tb00327.x>.
  24. Tsai MM, Fu YH, Deonier RC. 1990. Intrinsic bends and integration host factor binding at F plasmid *oriT*. *J Bacteriol* 172:4603–4609. <https://doi.org/10.1128/jb.172.8.4603-4609.1990>.
  25. Ziegelin G, Pansegrau W, Lurz R, Lanka E. 1992. TraK protein of conjugative plasmid RP4 forms a specialized nucleoprotein complex with the transfer origin. *J Biol Chem* 267:17279–17286.
  26. Zhang S, Meyer R. 1997. The relaxosome protein MobC promotes conjugal plasmid mobilization by extending DNA strand separation to the nick site at the origin of transfer. *Mol Microbiol* 25:509–516. <https://doi.org/10.1046/j.1365-2958.1997.4861849.x>.
  27. Lee CA, Babic A, Grossman AD. 2010. Autonomous plasmid-like replication of a conjugative transposon. *Mol Microbiol* 75:268–279. <https://doi.org/10.1111/j.1365-2958.2009.06985.x>.
  28. Thomas J, Lee CA, Grossman AD. 2013. A conserved helicase processivity factor is needed for conjugation and replication of an integrative and conjugative element. *PLoS Genet* 9:e1003198. <https://doi.org/10.1371/journal.pgen.1003198>.
  29. Fekete RA, Frost LS. 2002. Characterizing the DNA contacts and cooperative binding of F plasmid TraM to its cognate sites at *oriT*. *J Biol Chem* 277:16705–16711. <https://doi.org/10.1074/jbc.M111682200>.
  30. Nelson WC, Howard MT, Sherman JA, Matson SW. 1995. The *traY* gene product and integration host factor stimulate *Escherichia coli* DNA helicase I-catalyzed nicking at the F plasmid *oriT*. *J Biol Chem* 270: 28374–28380. <https://doi.org/10.1074/jbc.270.47.28374>.
  31. Ziegelin G, Fürste JP, Lanka E. 1989. TraJ protein of plasmid RP4 binds to a 19-base pair invert sequence repetition within the transfer origin. *J Biol Chem* 264:11989–11994.
  32. Moncalián G, Grandoso G, Llosa M, de la Cruz F. 1997. *oriT*-processing and regulatory roles of TrwA protein in plasmid R388 conjugation. *J Mol Biol* 270:188–200. <https://doi.org/10.1006/jmbi.1997.1082>.
  33. Rocco JM, Churchward G. 2006. The integrase of the conjugative transposon Tn916 directs strand- and sequence-specific cleavage of the origin of conjugal transfer, *oriT*, by the endonuclease Orf20. *J Bacteriol* 188:2207–2213. <https://doi.org/10.1128/JB.188.6.2207-2213.2006>.
  34. Pansegrau W, Balzer D, Kruff V, Lurz R, Lanka E. 1990. *In vitro* assembly of relaxosomes at the transfer origin of plasmid RP4. *Proc Natl Acad Sci U S A* 87:6555–6559. <https://doi.org/10.1073/pnas.87.17.6555>.
  35. Parker C, Meyer RJ. 2007. The R1162 relaxase/primase contains two, type IV transport signals that require the small plasmid protein MobB. *Mol Microbiol* 66:252–261. <https://doi.org/10.1111/j.1365-2958.2007.05925.x>.
  36. Disqué-Kochem C, Dreiseikelmann B. 1997. The cytoplasmic DNA-binding protein TraM binds to the inner membrane protein TraD *in vitro*. *J Bacteriol* 179:6133–6137. <https://doi.org/10.1128/jb.179.19.6133-6137.1997>.
  37. Beaber JW, Hochhut B, Waldor MK. 2002. Genomic and functional analyses of SXT, an integrating antibiotic resistance gene transfer element derived from *Vibrio cholerae*. *J Bacteriol* 184:4259–4269. <https://doi.org/10.1128/jb.184.15.4259-4269.2002>.
  38. Wozniak RAF, Fouts DE, Spagnoletti M, Colombo MM, Ceccarelli D, Garriss G, Déry C, Burrus V, Waldor MK. 2009. Comparative ICE genomics: insights into the evolution of the SXT/R391 family of ICEs. *PLoS Genet* 5:e1000786. <https://doi.org/10.1371/journal.pgen.1000786>.
  39. Lawley TD, Gilmour MW, Gunton JE, Standeven LJ, Taylor DE. 2002. Functional and mutational analysis of conjugative transfer region 1 (Tra1) from the IncHI1 plasmid R27. *J Bacteriol* 184:2173–2180. <https://doi.org/10.1128/jb.184.8.2173-2180.2002>.
  40. Ceccarelli D, Daccord A, René M, Burrus V. 2008. Identification of the origin of transfer (*oriT*) and a new gene required for mobilization of the SXT/R391 family of integrating conjugative elements. *J Bacteriol* 190: 5328–5338. <https://doi.org/10.1128/JB.00150-08>.
  41. Daccord A, Ceccarelli D, Burrus V. 2010. Integrating conjugative elements of the SXT/R391 family trigger the excision and drive the mobilization of a new class of *Vibrio* genomic islands. *Mol Microbiol* 78: 576–588. <https://doi.org/10.1111/j.1365-2958.2010.07364.x>.
  42. Cabezon E, Sastre JI, de la Cruz F. 1997. Genetic evidence of a coupling role for the TraG protein family in bacterial conjugation. *Mol Gen Genet* 254:400–406. <https://doi.org/10.1007/s004380050432>.
  43. Carraro N, Rivard N, Burrus V, Ceccarelli D. 2017. Mobilizable genomic islands, different strategies for the dissemination of multidrug resistance and other adaptive traits. *Mob Genet Elements* 7:1–6. <https://doi.org/10.1080/2159256X.2017.1304193>.
  44. Humbert M, Huguet KT, Coulombe F, Burrus V. 2019. Entry exclusion of conjugative plasmids of the IncA, IncC, and related untyped incompatibility groups. *J Bacteriol* 201:e00731-18. <https://doi.org/10.1128/JB.00731-18>.
  45. Kiss J, Papp PP, Szabó M, Farkas T, Murányi G, Szakállas E, Olasz F. 2015. The master regulator of IncA/C plasmids is recognized by the *Salmonella* genomic island SGI1 as a signal for excision and conjugal transfer. *Nucleic Acids Res* 43:8735–8745. <https://doi.org/10.1093/nar/gkv758>.
  46. Murányi G, Szabó M, Olasz F, Kiss J. 2016. Determination and analysis of the putative AcaCD-responsive promoters of *Salmonella* genomic island 1. *PLoS One* 11:e0164561. <https://doi.org/10.1371/journal.pone.0164561>.
  47. Huguet KT, Rivard N, Garneau D, Palanee J, Burrus V. 2020. Replication of the *Salmonella* genomic island 1 (SGI1) triggered by helper IncC conjugative plasmids promotes incompatibility and plasmid loss. *PLoS Genet* 16:e1008965. <https://doi.org/10.1371/journal.pgen.1008965>.
  48. Morita D, Takahashi E, Morita M, Ohnishi M, Mizuno T, Miyoshi S-I, Dutta D, Ramamurthy T, Chowdhury G, Mukhopadhyay AK, Okamoto K. 2020. Genomic characterization of antibiotic resistance-encoding genes in clinical isolates of *Vibrio cholerae* non-O1/non-O139 strains from Kolkata, India: generation of novel types of genomic islands containing plural antibiotic resistance genes. *Microbiol Immunol* 64:435–444. <https://doi.org/10.1111/1348-0421.12790>.
  49. Tenor JL, McCormick BA, Ausubel FM, Aballay A. 2004. *Caenorhabditis elegans*-based screen identifies *Salmonella* virulence factors required for conserved host-pathogen interactions. *Curr Biol* 14:1018–1024. <https://doi.org/10.1016/j.cub.2004.05.050>.
  50. Daccord A, Mursell M, Poulin-Laprade D, Burrus V. 2012. Dynamics of the SetCD-regulated integration and excision of genomic islands mobilized by integrating conjugative elements of the SXT/R391 family. *J Bacteriol* 194:5794–5802. <https://doi.org/10.1128/JB.01093-12>.
  51. Hochhut B, Marrero J, Waldor MK. 2000. Mobilization of plasmids and chromosomal DNA mediated by the SXT element, a *constin* found in *Vibrio cholerae* O139. *J Bacteriol* 182:2043–2047. <https://doi.org/10.1128/jb.182.7.2043-2047.2000>.
  52. Arteaga M, Velasco J, Rodriguez S, Vidal M, Arellano C, Silva F, Carreño LJ, Vidal R, Montero DA. 2020. Genomic characterization of the non-O1/non-O139 *Vibrio cholerae* strain that caused a gastroenteritis outbreak in Santiago, Chile, 2018. *Microb Genom* 6:e000340. <https://doi.org/10.1099/mgen.0.000340>.
  53. Ali M, Nelson AR, Lopez AL, Sack DA. 2015. Updated global burden of cholera in endemic countries. *PLoS Negl Trop Dis* 9:e0003832. <https://doi.org/10.1371/journal.pntd.0003832>.
  54. Escobar LE, Ryan SJ, Stewart-Ibarra AM, Finkelstein JL, King CA, Qiao H, Polhemus ME. 2015. A global map of suitability for coastal *Vibrio cholerae* under current and future climate conditions. *Acta Trop* 149:202–211. <https://doi.org/10.1016/j.actatropica.2015.05.028>.
  55. Vezzulli L, Grande C, Reid PC, Hélaouët P, Edwards M, Höfle MG, Brettar I, Colwell RR, Pruzzo C. 2016. Climate influence on *Vibrio* and associated human diseases during the past half-century in the coastal North Atlantic. *Proc Natl Acad Sci U S A* 113:E5062–E5071. <https://doi.org/10.1073/pnas.1609157113>.
  56. Kaper JB, Morris JG, Levine MM. 1995. Cholera. *Clin Microbiol Rev* 8:48–86. <https://doi.org/10.1128/CMR.8.1.48-86.1995>.
  57. Hasan NA, Choi SY, Eppinger M, Clark PW, Chen A, Alam M, Haley BJ, Taviani E, Hine E, Su Q, Tallon LJ, Prosper JB, Furth K, Hoq MM, Li H, Fraser-Liggett CM, Cravioto A, Huq A, Ravel J, Cebula TA, Colwell RR. 2012. Genomic diversity of 2010 Haitian cholera outbreak strains. *Proc*

- Natl Acad Sci U S A 109:E2010–E2017. <https://doi.org/10.1073/pnas.1207359109>.
58. Bik EM, Gouw RD, Mooi FR. 1996. DNA fingerprinting of *Vibrio cholerae* strains with a novel insertion sequence element: a tool to identify epidemic strains. *J Clin Microbiol* 34:1453–1461. <https://doi.org/10.1128/JCM.34.6.1453-1461.1996>.
  59. Li M, Shimada T, Morris JG, Sulakvelidze A, Sozhamannan S. 2002. Evidence for the emergence of non-O1 and non-O139 *Vibrio cholerae* strains with pathogenic potential by exchange of O-antigen biosynthesis regions. *Infect Immun* 70:2441–2453. <https://doi.org/10.1128/iai.70.5.2441-2453.2002>.
  60. Dalsgaard A, Serichantalergs O, Forslund A, Lin W, Mekalanos J, Mintz E, Shimada T, Wells JG. 2001. Clinical and environmental isolates of *Vibrio cholerae* serogroup O141 carry the CTX phage and the genes encoding the toxin-coregulated pili. *J Clin Microbiol* 39:4086–4092. <https://doi.org/10.1128/JCM.39.11.4086-4092.2001>.
  61. Montero DA, Canto FD, Velasco J, Colello R, Padola NL, Salazar JC, Martin CS, Oñate A, Blanco J, Rasko DA, Contreras C, Puente JL, Scheutz F, Franz E, Vidal RM. 2019. Cumulative acquisition of pathogenicity islands has shaped virulence potential and contributed to the emergence of LEE-negative Shiga toxin-producing *Escherichia coli* strains. *Emerg Microbes Infect* 8:486–502. <https://doi.org/10.1080/22221751.2019.1595985>.
  62. Peacock SJ, Moore CE, Justice A, Kantzanou M, Story L, Mackie K, O'Neill G, Day NPJ. 2002. Virulent combinations of adhesin and toxin genes in natural populations of *Staphylococcus aureus*. *Infect Immun* 70:4987–4996. <https://doi.org/10.1128/iai.70.9.4987-4996.2002>.
  63. Deshpande LM, Fritsche TR, Moet GJ, Biedenbach DJ, Jones RN. 2007. Antimicrobial resistance and molecular epidemiology of vancomycin-resistant enterococci from North America and Europe: a report from the SENTRY antimicrobial surveillance program. *Diagn Microbiol Infect Dis* 58:163–170. <https://doi.org/10.1016/j.diagmicrobio.2006.12.022>.
  64. Dower WJ, Miller JF, Ragsdale CW. 1988. High efficiency transformation of *E. coli* by high voltage electroporation. *Nucleic Acids Res* 16:6127–6145. <https://doi.org/10.1093/nar/16.13.6127>.
  65. Miller JH. 1992. A short course in bacterial genetics: a laboratory manual and handbook for *Escherichia coli* and related bacteria. Cold Spring Harbor Laboratory Press, Cold Spring Harbor, NY.
  66. Altschul SF, Gish W, Miller W, Myers EW, Lipman DJ. 1990. Basic local alignment search tool. *J Mol Biol* 215:403–410. [https://doi.org/10.1016/S0022-2836\(05\)80360-2](https://doi.org/10.1016/S0022-2836(05)80360-2).
  67. Li W, Godzik A. 2006. Cd-hit: a fast program for clustering and comparing large sets of protein or nucleotide sequences. *Bioinformatics* 22:1658–1659. <https://doi.org/10.1093/bioinformatics/btl158>.
  68. Edgar RC. 2004. MUSCLE: multiple sequence alignment with high accuracy and high throughput. *Nucleic Acids Res* 32:1792–1797. <https://doi.org/10.1093/nar/gkh340>.
  69. Capella-Gutiérrez S, Silla-Martínez JM, Gabaldón T. 2009. trimAl: a tool for automated alignment trimming in large-scale phylogenetic analyses. *Bioinformatics* 25:1972–1973. <https://doi.org/10.1093/bioinformatics/btp348>.
  70. Kumar S, Stecher G, Li M, Knyaz C, Tamura K. 2018. MEGA X: Molecular Evolutionary Genetics Analysis across computing platforms. *Mol Biol Evol* 35:1547–1549. <https://doi.org/10.1093/molbev/msy096>.
  71. Guindon S, Dufayard J-F, Lefort V, Anisimova M, Hordijk W, Gascuel O. 2010. New algorithms and methods to estimate maximum-likelihood phylogenies: assessing the performance of PhyML 3.0. *Syst Biol* 59:307–321. <https://doi.org/10.1093/sysbio/syq010>.
  72. Jones DT, Taylor WR, Thornton JM. 1992. The rapid generation of mutation data matrices from protein sequences. *Comput Appl Biosci* 8:275–282. <https://doi.org/10.1093/bioinformatics/8.3.275>.
  73. Le SQ, Gascuel O. 2008. An improved general amino acid replacement matrix. *Mol Biol Evol* 25:1307–1320. <https://doi.org/10.1093/molbev/msn067>.
  74. Zuker M. 2003. Mfold web server for nucleic acid folding and hybridization prediction. *Nucleic Acids Res* 31:3406–3415. <https://doi.org/10.1093/nar/gkg595>.
  75. Datsenko KA, Wanner BL. 2000. One-step inactivation of chromosomal genes in *Escherichia coli* K-12 using PCR products. *Proc Natl Acad Sci U S A* 97:6640–6645. <https://doi.org/10.1073/pnas.120163297>.
  76. Grenier F, Matteau D, Baby V, Rodrigue S. 2014. Complete genome sequence of *Escherichia coli* BW25113. *Genome Announc* 2:e01038-14. <https://doi.org/10.1128/genomeA.01038-14>.
  77. Singer M, Baker TA, Schnitzler G, Deischel SM, Goel M, Dove W, Jaacks KJ, Grossman AD, Erickson JW, Gross CA. 1989. A collection of strains containing genetically linked alternating antibiotic resistance elements for genetic mapping of *Escherichia coli*. *Microbiol Rev* 53:1–24. <https://doi.org/10.1128/MMBR.53.1.1-24.1989>.
  78. Garriss G, Waldor MK, Burrus V. 2009. Mobile antibiotic resistance encoding elements promote their own diversity. *PLoS Genet* 5:e1000775. <https://doi.org/10.1371/journal.pgen.1000775>.
  79. Guzman LM, Belin D, Carson MJ, Beckwith J. 1995. Tight regulation, modulation, and high-level expression by vectors containing the arabinose *PBAD* promoter. *J Bacteriol* 177:4121–4130. <https://doi.org/10.1128/jb.177.14.4121-4130.1995>.
  80. Haldimann A, Wanner BL. 2001. Conditional-replication, integration, excision, and retrieval plasmid-host systems for gene structure-function studies of bacteria. *J Bacteriol* 183:6384–6393. <https://doi.org/10.1128/JB.183.21.6384-6393.2001>.
  81. Datta S, Costantino N, Court DL. 2006. A set of recombinering plasmids for gram-negative bacteria. *Gene* 379:109–115. <https://doi.org/10.1016/j.gene.2006.04.018>.
  82. Cherepanov PP, Wackernagel W. 1995. Gene disruption in *Escherichia coli*: TcR and KmR cassettes with the option of FLP-catalyzed excision of the antibiotic-resistance determinant. *Gene* 158:9–14. [https://doi.org/10.1016/0378-1119\(95\)00193-a](https://doi.org/10.1016/0378-1119(95)00193-a).
  83. Doublet B, Douard G, Targant H, Meunier D, Madec J-Y, Clockaert A. 2008. Antibiotic marker modifications of lambda Red and FLP helper plasmids, pKD46 and pCP20, for inactivation of chromosomal genes using PCR products in multidrug-resistant strains. *J Microbiol Methods* 75:359–361. <https://doi.org/10.1016/j.mimet.2008.06.010>.